Bilge International Journal of Science and Technology Research

Web : http://dergipark.gov.tr/bilgesci - **E-mail:** kutbilgescience@gmail.com

Received: 12.02.2018
Accepted: 08.03.2018
DOI: 10.30516/bilgesci.393717

ISSN: 2587-0742
e-ISSN: 2587-1749
2(1), 74-82, 2018

Infrared and NMR Spectral Analyses and Computational Studies of 2-amino-3-methylbenzoic Acid

Muhammet Hakkı Yıldırım[1*]

Abstract: Detailed infrared spectrum in gas phase, NMR spectra analyses and theoretical studies of 2-amino-3-methylbenzoic acid were performed with DFT/B3LYP/6-311G+(2d,p) level of method in Gaussian 09W. Ground state molecular geometries of monomeric and dimeric structures were calculated in vacuum and compared to the experimental XRD results. Potential energy surface graphics of the proton transfer and torsional tautomerism process were obtained. Also, HOMA aromaticity chancing graphics were drowned in mentioned process. The IR band assignments and the decompositions of potential energy for each band were done using theoretical calculations. ^{1}H and ^{13}C NMR chemical shifts analyses were performed by using GIAO NMR calculations with SCRF solvent model.

Keywords: Anthranilic acid, FT-IR, NMR, DFT, HOMA analysis

1. Introduction

Anthranilic or aminobenzoic acid and its derivatives are used as a starting material for biological and chemical active material synthesis. Gichner et al. showed that the antimutagenic capacities of 2-, 3-, 4-aminobenzoic compounds depend on the location of amino group (Gichner et al., 1994). Detailed vibrational spectrum analysis and molecular characterizations with theoretical calculations of mentioned compounds were done by Samsonowicz et al. (Samsonowicz et al., 2005). Syahrani et al. reported that the biotransformation and structure elucidation of some aminobenzoic acid compound in suspension cultures of S. mammosum (Syahrani et al., 1999). The effect of p-aminobenzoic acid on the uptake of thymidine and uracil by Escherichia coli was published by Richards and Xing (Richards and Xing, 1995). X Ray crystal structure of title compound was published by Brown et al. (Brown and Marsh, 1963). Newman et al. obtained 3 Methylbenzyne from the reaction of 2-amino-3-methylbenzoic acid with 2-hydroxyiminoacet-o-toluidide (Newman and Kannan, 1976). Gerber et al. published synthesis and crystal structure a Rhenium(V) metal complex which is obtained from the reaction of the cis ReO_2^+ core with 2-amino-3-methylbenzoic acid (Gerber et al., 2003). Dong et al. prepared biological active compounds by using 2-amino-3-methylbenzoic acid (Dong et al., 2009).

Spectroscopic characterization with supported computational studies of organic compounds attract attention of researchers. Computational studies help us to better understand electronic properties of compounds, such as HOMO-LUMO (Öztürk and Gökçe, 2017), NLO (Eryılmaz et al., 2016), tautomeric equilibrium (Yıldırım et al., 2016) and prototropy (Albayrak Kaştaş et al., 2017). As a part of our ongoing studies about the derivatives of aminobenzoic acid (Yıldırım et al., 2015), we report spectroscopic and theoretical studies of 2-amino-3-methylbenzoic acid. To our knowledge, there is no study about its spectroscopic and computational characterization.

2. Material and Method

Initial geometry for optimization was directly taken from X-RD results (Brown and Marsh, 1963). All the calculations were performed on Gaussian 09W

[1]Giresun University, Dereli Vocational School, 28950, Giresun, Turkey
*Corresponding author: hakki.yildirim@giresun.edu.tr

Citation: Yıldırım, M. H. (2018). Infrared and NMR Spectral Analyses and Computational Studies of 2-amino-3-methylbenzoic Acid. Bilge International Journal of Science and Technology Research, 2 (1):74-82.

(Frisch et al., 2009) software with DFT theory. In the calculations, B3LYP hybrid functional (Becke, 1993) with 6-311G+(2d,p) basis set was used. For NMR calculations, GIAO method (Wolinski et al., 1990) was selected and solvent modelled with SCRF theory (Cossi et al., 2003; Tomasi et al., 2005). Because of title compound was found a dimeric structure in crystal phase, we performed the geometry optimizations for monomeric and dimeric structures.

3. Results and Discussions

3.1. Molecular structure

Optimized molecular structure with atom labeled scheme was given in Figure 1 and intra-molecular hydrogen bonds were presented with dashed lines.

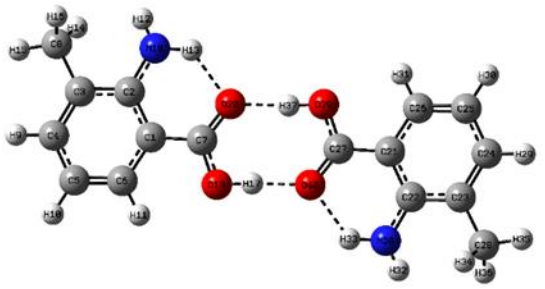

Figure 1. Optimized dimeric structure

To measure our computational level accuracy, experimental XRD and calculated bond lengths and angles were compared and a summary given in Table 1. Root mean square error values given in table were calculated for all bond lengths and angles.

As seen in Table 1, a good correlation can be found in between both monomeric and dimeric structure with the experimental one. The biggest differences between the experimental and calculated structure were occurred at atoms involved in a hydrogen bond. In the amino group, N-H bond lengths are found 0.88Å-0.91Å for x-ray while 1.01Å-1.00Å for calculated structure. Similarly, C7-O19-H17 bond angle was found 105.8° for monomeric structure while 110.2° for dimeric structure. In the inter-molecular hydrogen bond, hydrogen acceptor distance was 1.73Å for XRD while 1.66Å for dimeric structure. To make an overall comparison, the Root Mean Square Errors (RMSE) were given in Table 1. In the bond length, RMSE was 0.014 Å for both monomer and dimer structures, nearly equal to XRD deviation limit. 0.3° values were founded for angles showed that perfect match between the XRD and simulated structure, the exception of the C-O-H bond angle. Consequently, calculations of molecular structure are very successful when considering experimental values are taken in crystal structure while calculated values are taken in vacuum media

Table 1. A comparison table of geometric bond parameters of 2-amino-3-methylbenzoic acid

Bond Lengths (Å)	Exp.*	Monomer	Dimer
C7-O20	1.24	1.22	1.24
C7-O19	1.32	1.36	1.32
O19-H17	0.93	0.97	1.00
C2-N18	1.37	1.37	1.37
N18-H13	0.88	1.01	1.01
N18-H12	0.91	1.00	1.00
H17-O40	1.73	-	1.66
H13···O20	2.05	1.91	1.91
O19···O40	2.65	-	2.66
RMSE**		0.014	0.014
Bond Angles (°)			
C7-O19-H17	108.1	105.8	110.2
C1-C7-O19	114.7	114.0	115.1
C1-C7-O20	124.5	126.2	123.7
O19-C7-O20	120.8	119.8	121.2
C7-C1-C2	121.5	120.4	121.5
O19-H17···O40	170.0		176.7
N18-H13···O20	131.0	130.9	130.3
RMSE**		0.30	0.28
Dihedral Angles(°)			
O20-C7-O19-H17	1.3	0.0	0.0
C1-C7-O19-H17	-179.1	179.7	179.6
C3-C2-N18-H12	-7.2	-15.8	-16.4
O20-C7-C1-C6	176.9	178.3	178.1
O19-C7-C1-C2	177.9	179.4	179.2
RMSE**		0.37	0.39

*(Brown and Marsh, 1963), **Calculated for the all parameters

There is well-known fact that, 2-aminobenzoic acid derivatives show two type transformations which are the proton exchange in dimers (Monte and Hillesheim, 2001) and the rotation of carboxyl acid group (Fleisher et al., 2011). To find energy gap values between these transformations, relaxed potential energy surface scan calculations were performed. In dimeric structure, O19-H17···O40 pathway selected as a redundant coordinate for a relaxed scan calculation and proton was migrated of 0.05 Å step size.

Relative energies were calculated with respect to minimum energy and obtained potential energy

graphic was presented in Figure 2. Total energy of the dimer increased after the proton transfer process because of chancing structure of N-H···O intra-molecular hydrogen bond. Potential energy barrier for this transformation was found as 7.00 kcal/mol.

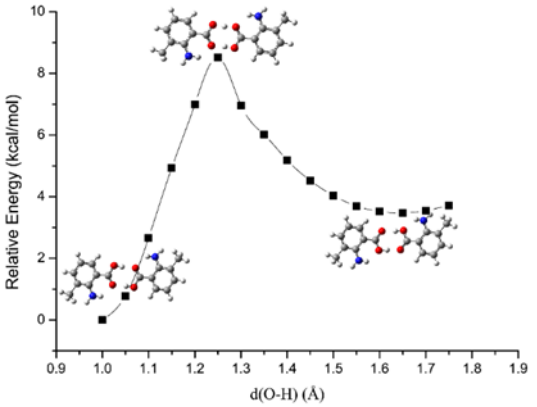

Figure 2. A relative energy graph for the proton transfer

Aromaticity indices were used to better understand the movement of π electrons in the ring. Bond parameter based aromaticity criteria was introduced by Kruszewski and Krygowski as HOMA (Harmonic Oscillator Model of Aromaticity). HOMA index of a ring is calculated by using the following equation:

$$HOMA = 1 - \frac{1}{n}\sum_{i=1}^{n} \alpha_i \left(R_i - R_{i,opt}\right)^2 \qquad (1)$$

where n is the number of bonds in the ring, αi is a normalization constant, R_i is the bond length and $R_{i,opt}$ optimized bond length (Kruszewski and Krygowski, 1972). For the aromatic ring, HOMA value is expected in the range of 0.90-0.99 while for non-aromatic ring is in the range of 0.50-0.80 (Krygowski, 1993). HOMA indices were calculated for each step of scan calculations and summarized in Figure 3.

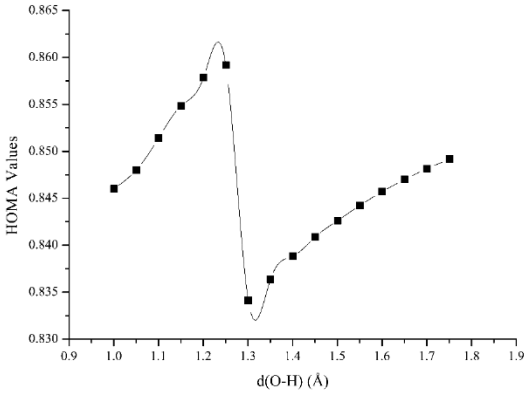

Figure 3. HOMA changing graphic during the proton transfer

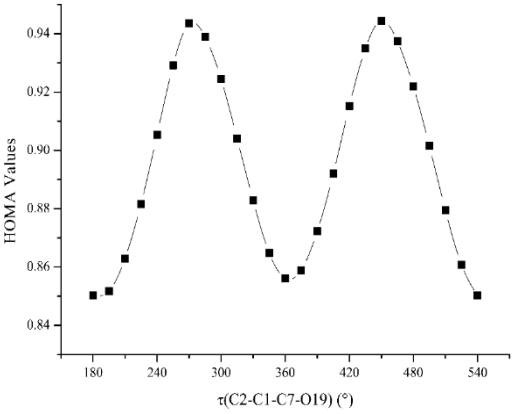

Figure 4. A torsional scan energy graph for the rotation

To draw a torsional potential energy profile for τ(C2-C1-C17-O19) torsion angle, a relaxed potential energy scan with the step size of 15° was done. Figure 4 represents the results of this scan calculation. Relative energies in the figure were calculated with respect to minimum energy.

As shown in Figure 4, the torsional energy barrier is 12.68 kcal/mol. Also, the transformation of intra-molecular hydrogen bond from NH-O to NH OH form increases the total energy by 3.23 kcal/mol. Also HOMA values are wagging to parallel of energy changing, as given in Figure 5.

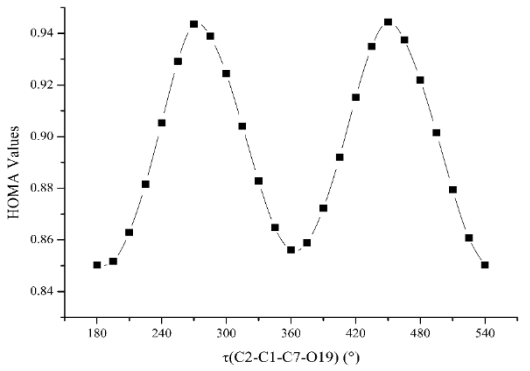

Figure 5. HOMA changing graphic during the proton transfer

3.2. Infrared spectroscopy analysis

Experimental gas phase IR spectrum data of the title compound were obtained from NIST Chemistry WebBook (Linstrom and Mallard, 2001) website. Due to overestimation problems of DFT calculations, calculated IR wavenumbers were scaled with two scale factor; 0.989 for lower than 1600 cm^{-1} and 0.954 for higher than 1600 cm^{-1} as in Wangs' study (Wang et al., 2015). Experimental and calculated monomeric and dimeric IR spectra which were obtained in gas phase were given in Figure 6.

Due to the experimental IR spectrum was recorded in 4000-600 cm^{-1}, Figure 1(a) has an interruption at 600-400 cm^{-1} region. As seen in figure, there is a good coherence between the experimental and calculated spectra. Therefore, band assignments with calculation of their PED values were made by VEDA (Jamróz, 2013) software and the results were given in Table 2, comparatively.

Hydroxyl group stretching vibration peak has been located at 3584 cm^{-1} and calculated as 3595 cm^{-1}. The experimental peaks at 3520 cm^{-1} and 3383 cm^{-1} can be attributed to symmetric and asymmetric stretching vibrations of amino group. Theoretical values of amino group stretching vibrations are 3531 cm^{-1} 3368 cm^{-1}. Aromatic C-H stretching vibrations are found at 3085 cm^{-1}, 3049 cm^{-1} and 3017 cm^{-1} in the experimental spectrum while their calculated values are 3065 cm^{-1}, 3041 cm^{-1}, 3011 cm^{-1}. Methyl group stretching vibrations are in the region of 2982-2879 cm^{-1}. The most intense peak (1725 cm^{-1}) in the spectrum corresponds to the C=O stretching vibration. This peak caused maximum deviation between the experimental and calculated spectra with $\Delta\nu$ is 75 cm^{-1}, which may be originated from steric effect in gas phase. Other intense peaks founded at 1166 cm^{-1} and 1079 cm^{-1} arise from in-plane and out of plane vibrations of hydroxyl group (Gardner and Wright, 2011).

Comparing to the IR spectrum of 2-aminobenzoic acid in solid phase (Samsonowicz et al., 2005), the major shifts take place in the carboxyl group, due to the aminobenzoic acid derivatives prefer dimeric structure in solid state while IR spectrum of the title compound was obtained in gas phase. Stretching vibration of C=O group was assigned 1670 cm^{-1} for 2-aminobenzoic acid while 1725 cm^{-1} for the title compound. In the experimental spectrum of 2-amino-3-benzoic acid, the ν(C-N) vibration was found at 1319 cm^{-1}, which is calculated as 1307 cm^{-1}, while the same vibration was found at 1326 cm^{-1} for 2-aminobenzoic acid. ν(C-OH) vibration peak located at 1261 cm^{-1} (exp.) 1213 cm^{-1} (calc.) and 1253 cm^{-1} (2-aminobenzoic) acid.

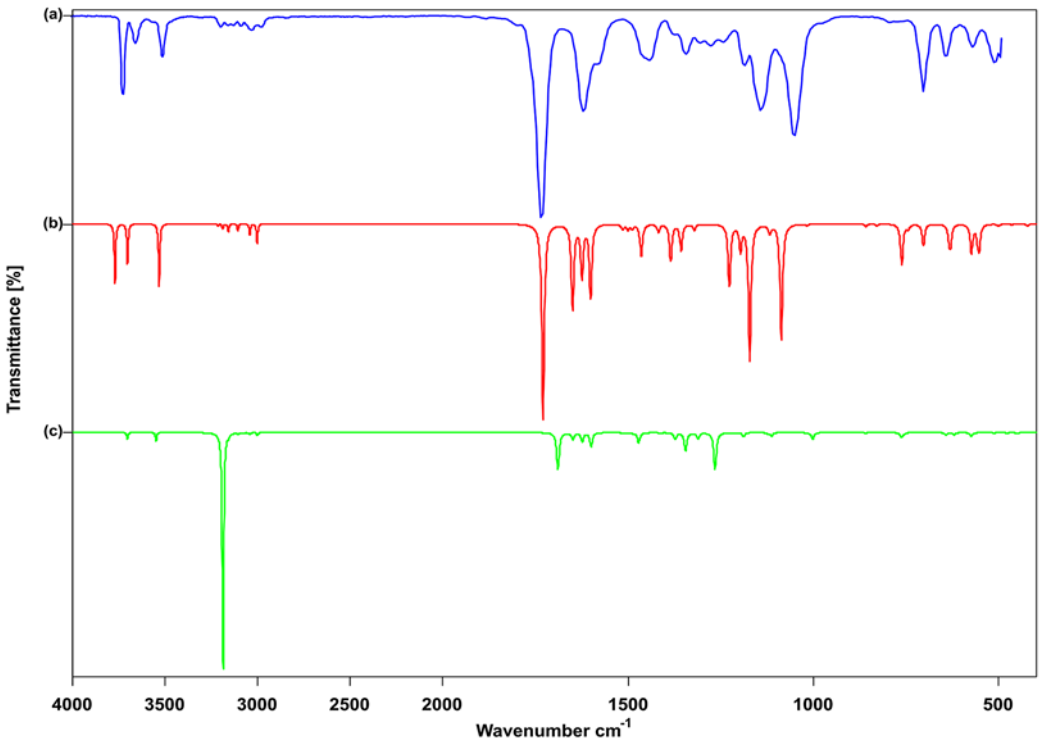

Figure 6. Experimental (a) and calculated monomeric (b), dimeric (c) gas phase IR spectra of the compound

Table 2. Infrared band assignments with their PED values of 2-amino-3-methylbenzoic acid

Exp. Freq	Calc. Freq.	Calc. Int.	Assignments with PED values (Only major contributions)
3584	3595	105	ν(O19-H17)(%100)
3520	3531	70	ν(N18-H12)(%84) + ν(N18-H13)(%15)
3383	3368	111	ν(N18-H12)(%15) + ν(N18-H13)(%84)
3085	3065	3	ν(C6-H11)(%91)
3047	3041	9	ν(C5-H10)(%85)
3019	3011	13	ν(C4-H9)(%93)
2982	2962	13	ν(C8-H15)(%91)
2929	2901	19	ν(C8-H14)(%35) + ν(C8-H16)(%64)
2879	2863	35	ν(C8-H14)(%62) + ν(C8-H16)(%30)
1725	1650	346	ν(O20-C7)(%68)
1618	1574	149	ν(C4-C3)(%12) + ν(C1-C6)(%14) +β(H13-N18-H12)(%26)
1582	1550	127	ν(C6-C5)(%14) + β(H13-N18-H12)(%31)
	1527	92	ν(C5-C4)(%16) + β(H13-N18-H12)(%19)
	1498	10	β(H14-C8-H16)(%29) + β(H15-C8-H14)(%13)
	1484	9	ν(C1-C6)(%12) + β(H9-C4-C5)(%10) +β(H10-C5-C6)(%22)
	1472	8	β(H15-C8-H14)(%38) + β(H16-C8-H15)(%42) +τ(H15-C8-C3-C4)(%12)
1449	1448	58	ν(N18-C2)(%17) + β(H11-C6-C1)(%10) +β(H14-C8-H16)(%14)
	1403	14	β(H14-C8-H16)(%32) + β(H15-C8-H14)(%25) +β(H16-C8-H15)(%28)
1384	1370	65	ν(C6-C5)(%12) + ν(O19-C7)(%13) +ν(C7-C1)(%14) +β(H17-O19-C7)(%15)
1355	1342	46	ν(C4-C3)(%20) + ν(C2-C3)(%10)
1319	1307	11	ν(N18-C2)(%20) + β(H9-C4-C5)(%31)
1292	1282	2	ν(C1-C6)(%20) + ν(N18-C2)(%12) +β(H11-C6-C1)(%25)
1261	1213	107	ν(C8-C3)(%24) + β(H17-O19-C7)(%13) +β(C1-C6-C5)(%10)
1206	1184	46	ν(C6-C5)(%11) + β(H17-O19-C7)(%10) +β(H10-C5-C6)(%41)
1166	1159	239	ν(O19-C7)(%13) + β(H17-O19-C7)(%20) +β(H12-N18-C2)(%14) +β(H10-C5-C6)(%11) + β(H11-C6-C1)(%12)
	1106	15	ν(C6-C5)(%22) + ν(C5-C4)(%27) +β(H9-C4-C5)(%20)
1079	1075	204	ν(O19-C7)(%33) + β(H12-N18-C2)(%25) +β(C1-C6-C5)(%13)
	1053	1	β(H15-C8-H14)(%11) + β(H16-C8-H15)(%11) +τ(H15-C8-C3-C4)(%55) +γ(C8-C4-C2-C3)(%10)
	1006	3	β(H14-C8-H16)(%10) + τ(H14-C8-C3-C4)(%27) +τ(H16-C8-C3-C4)(%26)
	963	0	τ(H10-C5-C6-C1)(%24) + τ(H11-C6-C1-C7)(%43) +τ(C1-C6-C5-C4)(%16)
	928	0	τ(H9-C4-C5-C6)(%53) + τ(H11-C6-C1-C7)(%26)
891	870	1	ν(C2-C3)(%13) + ν(O19-C7)(%13) +ν(C7-C1)(%13) +ν(C8-C3)(%20) + β(C5-C4-C3)(%10)
836	849	5	ν(N18-C2)(%14) + β(C2-C3-C4)(%10) +β(C6-C5-C4)(%35) +β(C5-C4-C3)(%14)
	820	3	τ(H10-C5-C6-C1)(%17) + γ(O20-C1-O19-C7)(%42) +γ(C7-C6-C2-C1)(%14) +γ(N18-C3-C1-C2)(%11)
750	753	72	τ(H9-C4-C5-C6)(%13) + τ(H10-C5-C6-C1)(%50) +τ(H11-C6-C1-C7)(%19)
	736	9	τ(C2-C3-C4-C5)(%14) + γ(O20-C1-O19-C7)(%29) +γ(N18-C3-C1-C2)(%22)
	696	20	β(O20-C7-O19)(%32)
624	627	37	β(O20-C7-O19)(%12) + τ(H13-N18-C2-C3)(%45)
599	623	34	β(O20-C7-O19)(%16) + β(C5-C4-C3)(%10) +τ(H13-N18-C2-C3)(%36)
	568	51	τ(H17-O19-C7-C1)(%52) + τ(C1-C6-C5-C4)(%11) +γ(N18-C3-C1-C2)(%13)
	551	16	β(O19-C7-C1)(%15) + τ(H17-O19-C7-C1)(%12)
	547	43	τ(H17-O19-C7-C1)(%19) + τ(C1-C6-C5-C4)(%16) +γ(N18-C3-C1-C2)(%10)
	496	4	ν(C8-C3)(%13) + β(C2-C3-C4)(%16) +β(C7-C1-C6)(%12)
	460	1	τ(H17-O19-C7-C1)(%13) + γ(C7-C6-C2-C1)(%16) +γ(C8-C4-C2-C3)(%22)
	418	3	β(N18-C2-C1)(%40) + β(O19-C7-C1)(%20)
	375	14	ν(C7-C1)(%18) + β(C6-C5-C4)(%11) +β(C1-C6-C5)(%24)
	346	5	β(O19-C7-C1)(%17) + β(C8-C3-C2)(%50)
	300	138	τ(H12-N18-C2-C3)(%56)
	266	6	τ(C6-C5-C4-C3)(%11) + γ(C7-C6-C2-C1)(%13) +γ(N18-C3-C1-C2)(%22) +γ(C8-C4-C2-C3)(%31)
	230	3	β(O19-C7-C1)(%19) + β(C7-C1-C6)(%49) +β(C8-C3-C2)(%12)
	204	10	τ(H14-C8-C3-C4)(%33) + τ(H15-C8-C3-C4)(%17) +τ(H16-C8-C3-C4)(%35)
	198	7	τ(C2-C3-C4-C5)(%35) + γ(C7-C6-C2-C1)(%19) +γ(C8-C4-C2-C3)(%13)
	106	1	τ(C6-C5-C4-C3)(%35) + τ(C1-C6-C5-C4)(%18) +τ(O19-C7-C1-C6)(%13) +γ(C7-C6-C2-C1)(%15)
	72	1	τ(O19-C7-C1-C6)(%77)
RMSE	25		

ν: Stretching, β: In-plane bending, τ: Torsion, γ: Out-of-plane bending

3.3. NMR analysis

Experimental ^{1}H and ^{13}C NMR spectra of 2-amino-3-methoxybenzoic acid were obtained from AIST database (AIST, 2017) which were sample saturated in DMSO-d6 and data acquired with an 89.56 MHz instrument. NMR chemical shifts of 2 aminobenzoic acid (Samsonowicz et al., 2005), 2-amino-3-methylbenzoic acid and calculated spectra were given in Table 3. In the experimental spectra of 2-amino-3-methylbenzoic acid, there was only a small shift on C3 atom, which methyl group is attached to C3, when compared to 2-aminobenzoic acid NMR spectra. On the other hand, there was a systematic small down-field shift in calculated spectra.

Table 3. Chemical shifts for 2-amino benzoic acid and 2-amino-3-methylbenzoic acid

Atom	δexp*	δexp**	δcalc
C1	109.69	109.39	109.89
C2	151.58	149.63	156.72
C3	114.69	122.91	128.37
C4	133.82	134.33	140.93
C5	116.42	114.27	117.56
C6	131.26	128.97	134.76
C7	169.69	169.96	176.16
C8		17.41	17.69
H9	7.21	7.16	7.56
H10	6.50	6.48	6.77
H11	7.70	7.63	8.11
H14, 15, 16	-	2.11	2.13

*2-aminobenzoic acid (Samsonowicz et al., 2005),
**2-amino-3-methylbenzoic acid (AIST, 2017)

These deviations can be reduced by using empirical scale factor proposed from Forsyth and Sebag (Forsyth and Sebag, 1997), but in this case was not necessary. Due to carboxyl and amino protons are constantly changing from one atom to another atom in solvent media, their proton NMR peaks are generally broad or lose (Anderson et al., 2004). Moreover, their shifts are depending on the solvent, concentration and temperature. Therefore, their peaks could not be assigned as in 2 aminobenzoic acid compound (Samsonowicz et al., 2005).

4. Conclusions

Geometry optimizations of title compound show a good agreement with experimental XRD values. Potential energy scan calculations with HOMA aromaticity index chancing graphics were obtained. Therefore, we decided to the selected theoretical method was sufficient. 2-amino-3-benzoic acid consists of 20 atoms which has 54 normal modes from 3N-6 rule. All the normal modes were assigned with their PED values. NMR spectra chemical shifts were not fully resolved due to the nature of both acidic and basic group included in the compound.

References

AIST, (2017). National Institute of Advanced Industrial Science and Technology Spectral Database for Organic Compounds, SDBS. http://sdbs.db.aist.go.jp/sdbs/ (Accessed on: 09.09.2017).

Albayrak Kaştaş, Ç., Kaştaş, G., Güder, A., Gür, M., Muğlu, H., Büyükgüngör, O. (2017). Investigation of two o -hydroxy Schiff bases in terms of prototropy and radical scavenging activity. Journal of Molecular Structure, 1130: 623–632.

Anderson, R.J., Bendell, D.J., Groundwater, P.W. (2004). Nuclear magnetic resonance spectroscopy. Abel, E.W. (Ed.) Organic Spectroscopic Analysis. Cambridge, England.

Becke, A.D. (1993). Density-functional thermochemistry. III. The role of exact exchange. The Journal of Chemical Physics, 98(7): 5648.

Brown, G.M., Marsh, R.E. (1963). The crystal and molecular structure of 2-amino-3-methylbenzoic acid. Acta Crystallographica, 16(3): 191–202.

Cossi, M., Rega, N., Scalmani, G., Barone, V. (2003). Energies, structures, and electronic properties of molecules in solution with the C-PCM solvation model. Journal of Computational Chemistry, 24(6): 669–681.

Dong, W., Xu, J., Xiong, L., Liu, X., Li, Z. (2009). Synthesis, structure and biological activities of some novel anthranilic acid esters containing N-Pyridylpyrazole. Chinese Journal of Chemistry, 27(3): 579–586.

Eryılmaz, S., Gül, M., İnkaya, E., İdil, Ö., Özdemir, N. (2016). Synthesis, crystal structure analysis, spectral characterization, quantum chemical calculations, antioxidant and antimicrobial activity of 3-(4-chlorophenyl)-3a,4,7,7a-tetrahydro-4,7-

methanobenzo[d]isoxazole. Journal of Molecular Structure, 1122: 219–233.

Fleisher, A.J., Morgan, P.J., Pratt, D.W. (2011). High-Resolution electronic spectroscopy studies of meta-aminobenzoic acid in the gas phase reveal the origins of its solvatochromic behavior. ChemPhysChem, 12(10): 1808–1815.

Forsyth, D.A., Sebag, A.B. (1997). Computed 13C NMR chemical shifts via empirically scaled GIAO shieldings and molecular mechanics geometries. Conformation and configuration from 13C shifts. Journal of the American Chemical Society, 119(40): 9483–9494

Frisch, M.J., Trucks, G.W., Schlegel, H.B., Scuseria, G.E., Robb, M.A., Cheeseman, J.R., Scalmani, G., Barone, V., Mennucci, B., Petersson, G.A., Nakatsuji, H., Caricato, M., Li, X., Hratchian, H.P., Izmaylov, A.F., Bloino, J., Zheng, G., Sonnenberg, J.L., Hada, M., Ehara, M., Toyota, K., Fukuda, R., Hasegawa, J., Ishida, M., Nakajima, T., Honda, Y., Kitao, O., Nakai, H., Vreven, T., Montgomery Jr., J.A., Peralta, J.E., Ogliaro, F., Bearpark, M., Heyd, J.J., Brothers, E., Kudin, K.N., Staroverov, V.N., Kobayashi, R., Normand, J., Raghavachari, K., Rendell, A., Burant, J.C., Iyengar, S.S., Tomasi, J., Cossi, M., Rega, N., Millam, J.M., Klene, M., Knox, J.E., Cross, J.B., Bakken, V., Adamo, C., Jaramillo, J., Gomperts, R., Stratmann, R.E., Yazyev, O., Austin, A.J., Cammi, R., Pomelli, C., Ochterski, J.W., Martin, R.L., Morokuma, K., Zakrzewski, V.G., Voth, G.A., Salvador, P., Dannenberg, J.J., Dapprich, S., Daniels, A.D., Farkas, Ö., Foresman, J.B., Ortiz, J.V., Cioslowski, J., Fox, D.J. (2009). Gaussian 09, Revision C.01, Gaussian, Inc., Wallingford CT.

Gardner, A.M., Wright, T.G. (2011). Consistent assignment of the vibrations of monosubstituted benzenes. Journal of Chemical Physics, 135(11): 1–18.

Gerber, T.I.A., Luzipo, D., Mayer, P. (2003). The Reaction of the cis -ReO_2^+ core with 2-amino-3-methylbenzoic acid. Journal of Coordination Chemistry, 56(18): 1549–1554.

Gichner, T., Voutsinas, G., Patrineli, A., Kappas, A., Plewa, M.J. (1994). Antimutagenicity of three isomers of aminobenzoic acid in Salmonella typhimurium. Mutation Research/Fundamental and Molecular Mechanisms of Mutagenesis, 309(2): 201–210.

Jamróz, M.H. (2013). Vibrational Energy Distribution Analysis (VEDA): Scopes and limitations. Spectrochimica Acta Part A: Molecular and Biomolecular Spectroscopy, 114: 220–230.

Kruszewski, J., Krygowski, T.M. (1972). Definition of aromaticity basing on the harmonic oscillator model. Tetrahedron Letters, 13(36): 3839–3842.

Krygowski, T.M. (1993). Crystallographic studies of inter- and intramolecular interactions reflected in aromatic character of pi-electron systems. Journal of Chemical Information and Modeling, 33(1): 70–78.

Linstrom, P.J., Mallard, W.G. (2001). NIST Chemistry webbook; NIST standard reference database No. 69. NIST Chemistry WebBook, (69): 20899.

Monte, M.J.S., Hillesheim, D.M. (2001). Thermodynamic study of the sublimation of six aminomethylbenzoic acids. The Journal of Chemical Thermodynamics, 33(7): 745–754.

Newman, M.S., Kannan, R. (1976). Reactions of 3-methylbenzyne with 2-substituted furans. Steric effects. The Journal of Organic Chemistry, 41(21): 3356–3359.

Öztürk, N., Gökçe, H. (2017). Structural and spectroscopic (FT-IR and NMR) analyses on (E)-pent-2-enoic acid. Bilge International Journal of Science and Technology Research, 1(1): 9–15.

Richards, M.R.E., Xing, D.K.L. (1995). The effect of p-aminobenzoic acid on the uptake of thymidine and uracil by Escherichia coli. International Journal of Pharmaceutics, 116(2): 217–221.

Samsonowicz, M., Hrynaszkiewicz, T., Świsłocka, R., Regulska, E., Lewandowski, W. (2005). Experimental and theoretical IR, Raman, NMR spectra of 2-, 3- and 4-aminobenzoic acids. Journal of Molecular Structure, 744(2005): 345–352.

Syahrani, A., Ratnasari, E., Indrayanto, G., Wilkins, A. (1999). Biotransformation of o-and p-aminobenzoic acids and N-acetyl p-aminobenzoic acid by cell suspension

cultures of Solanum. Phytochemistry, 51(5): 615–620.

Tomasi, J., Mennucci, B., Cammi, R. (2005). Quantum mechanical continuum solvation models. Chemical Reviews, 105(8): 2999–3094.

Wang, Z., Chen, J., Li, L., Zhou, Z., Geng, Y., Sun, T. (2015). Detailed structural study of β-artemether: Density functional theory (DFT) calculations of Infrared, Raman spectroscopy, and vibrational circular dichroism. Journal of Molecular Structure, 1097: 61–68.

Wolinski, K., Hinton, J.F., Pulay, P. (1990). Efficient implementation of the gauge-independent atomic orbital method for NMR chemical shift calculations. Journal of the American Chemical Society, 112(23): 8251–8260.

Yıldırım, A.Ö., Yıldırım, M.H., Kaştaş, Ç.A. (2016). Studies on the synthesis, spectroscopic analysis and DFT calculations on (E) 4,6 dichloro 2 [(2 chlorophenylimino) methyl] 3 methoxyphenol as a novel Schiff's base. Journal of Molecular Structure, 1113: 1–8.

Yıldırım, M.H., Paşaoğlu, H., Odabaşoğlu, H.Y., Odabaşoğlu, M., Yıldırım, A.Ö. (2015). Synthesis, structural and computational characterization of 2-amino-3,5-diiodobenzoic acid and 2-amino-3,5-dibromobenzoic acid. Spectrochimica Acta Part A: Molecular and Biomolecular Spectroscopy, 146: 50–60.